

80-2-264
高

DEUTSCHES ELEKTRONEN-SYNCHROTRON **DESY**

DESY 80/06
January 1980

MULTIGLUON EFFECTS AND $\langle p_T^2 \rangle$ IN e^+e^- -ANNIHILATION

by

F. Gutbrod

NOTKESTRASSE 85 · 2 HAMBURG 52

To be sure that your preprints are promptly included in the
HIGH ENERGY PHYSICS INDEX ,
send them to the following address (if possible by air mail) :

DESY
Bibliothek
Notkestrasse 85
2 Hamburg 52
Germany

DESY 80/06
January 1980

Multigluon effects and $\langle p_T^2 \rangle$ in e^+e^- -annihilation

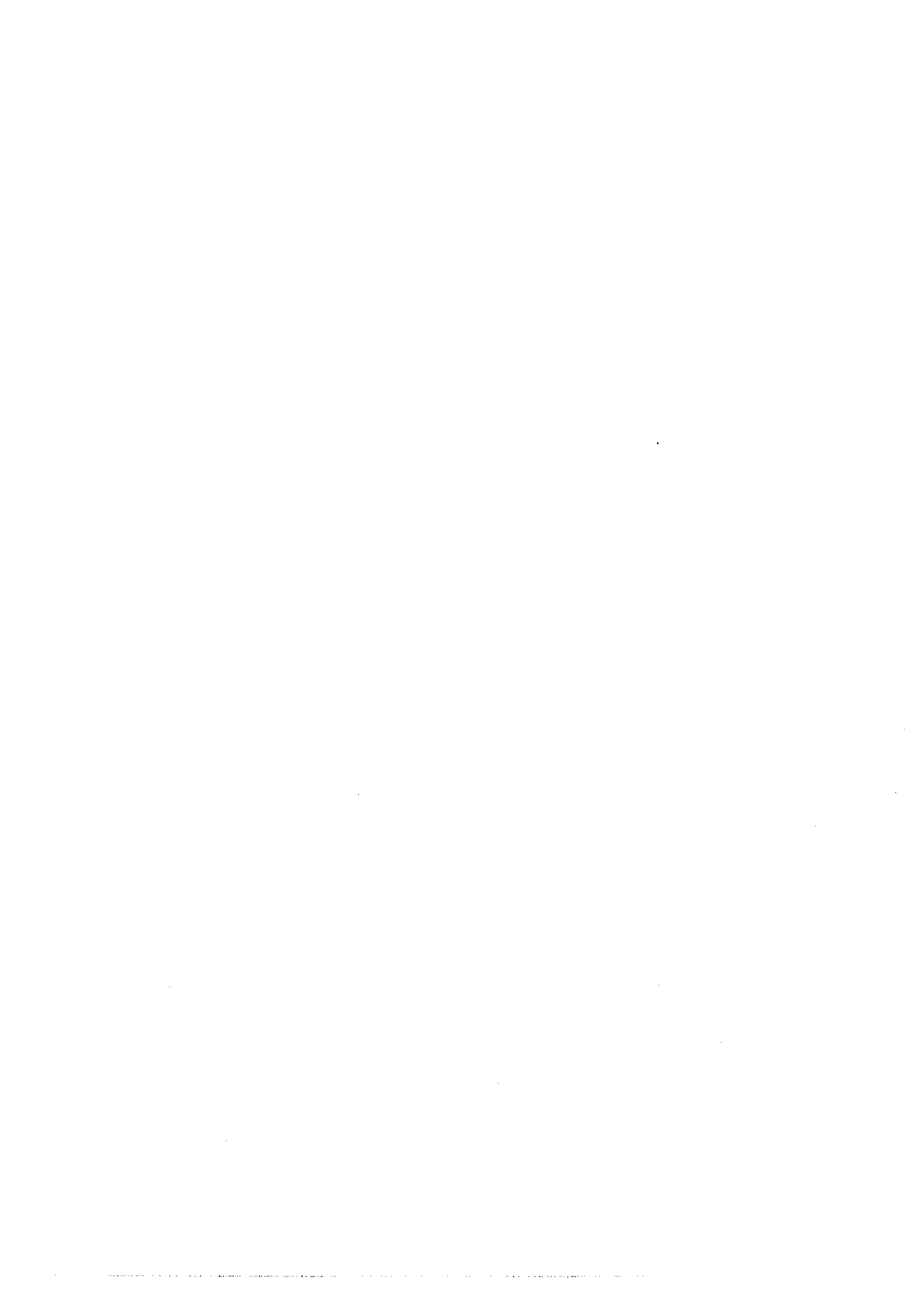
by

F. Gutbrod

Deutsches Elektronen-Synchrotron DESY, Hamburg

Abstract

The average transverse momentum of quarks and hadrons in e^+e^- -annihilation is calculated in the ladder approximation. The planar gauge is used with correct kinematics. The theoretical results for $\langle p_T^2 \rangle$ are well above the lowest order calculation, if this is performed with a large cut-off mass.



1. Introduction

The broadening of hadronic jets or the growth of hadronic transverse momenta with respect to the jet axis is presently of central interest in leptonic processes, especially in e^+e^- annihilation (1-4). The details of this broadening may provide a quantitative test for QCD, and recent calculations (5) based on the first order in the strong coupling constant α_s are in agreement with many properties of annihilation events found at PETRA (1,2). It is, however, well known that the underlying process, namely gluon bremsstrahlung from quarks, has a small probability only with special cut-off procedures (these are kinematical criterions under which gluon bremsstrahlung events are disregarded). E.g. the thrust cut-off (5) corresponds, at a CMS-energy of $\sqrt{q^2} = 30$ GeV, to a lower cut-off in jet masses of $M_0 = 6.7$ GeV. It is to be expected that theoretical predictions for average quantities [†] like the hadronic squared transverse momenta $\langle p_T^2 \rangle$ with respect to the jet axis depend on M_0 . It cannot be taken much lower than the above value as then the $O(\alpha_s)$ approximation becomes meaningless. On the other hand a scale of 6.7 GeV as the point of breakdown of perturbation theory is not in line with the application of QCD to deep inelastic processes at $|q^2| \lesssim 100$ GeV², where the internal momentum transfers are considerably smaller than the external q^2 . To overcome the difficulty with M_0 , we adopt the hypothesis that the large terms in the perturbation expansion, which are of the form $\frac{\alpha_s}{\pi} \ln \frac{q^2}{M_0^2}$ and $\frac{\alpha_s}{\pi} \ln^2 \frac{q^2}{M_0^2}$, are summable or cancel in a transparent way down to M_0 internal momenta of order $k^2 \gtrsim M_0^2 \approx 1$ GeV². It is known on the level of leading logarithmic

[†] Calculated rates for clean, i.e. large angle three jet events are probably insensitive to M_0 .

accuracy (LLA) that this summation is possible in terms of dressed tree diagrams (6). We attempt here to extract from a sum of special tree diagrams predictions for the average p_T^2 of hadrons in e^+e^- annihilation jets and compare them to the $O(\alpha_s)$ results.

The full tree graph approximation should contain emission of gluons from the initial quark pair, gluon and quark pair emission from the secondary gluons and so on. For the sake of simplicity we shall neglect the second process, i.e. we consider only bremsstrahlung of real gluons from the quarks produced by the virtual photon, as indicated in fig. 1a. This is certainly a good approximation if we focus our attention to hadrons with large momenta, say $x \gtrsim 0.5$ ($x = 2E_{\text{hadron}}/\sqrt{q^2}$). The reason is that gluons are predominantly soft (they have small x), so especially after fragmentation into hadrons they do not populate the large x region.

In fig. 1b we graphically formulate the Bethe-Salpeter equation (BSE) for the quark or antiquark inclusive structure function, which we shall solve. It is assumed that interferences between various gluons can be neglected and that propagator and vertex corrections combine such that we can work with free internal propagators and the running coupling constant α_s at each vertex. By weighting the integral involved in the BSE with the squared transverse momentum (k_T^2) we can derive the average k_T^2 of quarks. An assumption about quark fragmentation leads to $\langle p_T^2 \rangle$ of hadrons in the final state. In the next section we write down and explain the BSE for gluon emission. Calculational details are given in section 3, and results for $\langle p_T^2 \rangle$ are presented for $\sqrt{q^2} = 12$ GeV and 30 GeV as functions of the energy of hadrons (so-called seagull plots). Section 4 contains conclusions.

2. The Bethe-Salpeter Equation

Our aim is to have a single twodimensional integral equation, which describes multi-gluon emission from one of the quarks created in e^+e^- annihilation. The necessary steps, namely selection of a suitable gauge, reduction of the spinor algebra in LLA, and infrared regularization are explained in (7) for ep-scattering. The formalism is easily adapted for $e^+e^- \rightarrow$ quark + anything. We here give only the final equation, discuss its physical origin and point out necessary modifications.

The object under study is the quark inclusive structure function $\bar{W}_1(x, k^2)$, where k is the quark momentum, and x is defined[†] by (see fig. 1b)

$$(q - k)^2 = q^2(1 - x) \tag{2.1}$$

For $k^2 = 0$, x agrees with the usual variable $2E_k/q \cdot \bar{W}_1(x, k^2)$ is related, under the assumption of negligible longitudinal cross section, to the inclusive quark production cross section by

$$\frac{d\sigma_A}{dx} = 2 \sigma_{\mu\nu} \times \bar{W}_1(x, k^2 = 0) \tag{2.2}$$

Here $\sigma_{\mu\nu}$ is the cross section for $e^+e^- \rightarrow \mu^+\mu^-$. In the following we consider directly the quantity

$$W(x, k^2) \equiv x \bar{W}_1(x, k^2). \tag{2.3}$$

In the special axial gauge, where the gluon propagator has the Lorentz

[†] No confusion should arise from our simultaneous use of x for quarks and for hadrons.

structure (1 = gluon momentum)

$$d_{\mu\nu} = -g_{\mu\nu} + \frac{q_\mu t_\nu + q_\nu t_\mu}{q \cdot l} - \frac{q^2 t_\mu t_\nu}{(q \cdot l)^2} \tag{2.4}$$

all interference terms between gluons coming from different places in the ladder and from different quarks can be neglected in the LLA. The sum of virtual gluon corrections organizes under (2.4) in the following way: The photon-quark vertex becomes a function of q^2 only. Infrared singular diagrams (singular for $k^2 \rightarrow 0$) are in the quark propagator, which in LLA reads (6)

$$S_F(k) = \frac{1}{k} d(k^2, x), \tag{2.5}$$

where the argument of the running coupling constant $\alpha_s(k^2)$ lies between k^2 and q^2 . The square of this and other nonleading propagator renormalizations combine (8) with the corrections of the vertex following the line k (away from the photon), together with the gluon propagator renormalization, to give the renormalized $\alpha_s(k^2)$.

One is then left with one renormalization factor $d(k^2 = 0, x)$ for external lines, the other being absorbed by the wave function renormalization. It will be cut-off dependent, as we have to explain below. The virtual corrections thus amount to an x -dependent external multiplicative renormalization. This is also the case in the probabilistic version (9) where the virtual corrections in lowest order have the form[†]

[†] The author is indebted to Dr. E. Pietarinen for pointing this out to him.

$$\int_{k^2}^{k'^2} \frac{dk^2}{k^2} \int_0^1 dz P(z, k, x) \quad (2.6)$$

(here $P(z, \kappa, x)$ = decay probability for quark \rightarrow quark + gluon) for a quark line of momentum k , which is the decay product of a quark k' . Linking all lines together one ends up with a x -dependent external renormalization.

Apart from this renormalization multi-gluon emission is described (7) by the BSE

$$W(x, k^2) = W_0(x, k^2) + \frac{2}{3\pi} \int_x^1 \frac{dx'}{x'} \int_{k_{min}^2}^{k_{max}^2} dk'^2 \frac{\alpha_s(k'^2)}{k'^2 + M_0^2} x \quad (2.7)$$

$$\times P(x, x', k^2, k'^2) W\left(\frac{x}{x'}, k'^2\right)$$

Let us start to explain (2.7) by defining the kernel $P(x, x', k^2, k'^2)$. It contains the spinorial part of the gluon emission probability in the axial gauge (2.4),

$$P(x, x', k^2, k'^2) = \frac{1 + Z^2}{1 - Z + \varepsilon} \quad (2.8)$$

with

$$\begin{aligned} Z &= \frac{k \cdot q}{k' \cdot q} \\ &= x' \frac{1 + k'^2/xq^2}{1 + x'k'^2/xq^2} \end{aligned} \quad (2.9)$$

The last term in (2.4) has been discarded as a k'^2/q^2 correction, which should not be kept in LL.A. The infrared regulator ε is necessary only in the kinematic region $k^2 \approx k'^2$. It should suppress gluons with energies of less than a few hundred MeV.

The other infrared regulator, M_0^2 , would be unnecessary if we would keep $k^2 > 0$ in (2.7) throughout. Since x and k^2 are not completely independent, we prefer to set $k^2 = 0$ at the end and fix M_0 as the mass down to which we trust our perturbative summation. The kinematical limit k_{max}^2 has to be evaluated accurately for a calculation of $\langle k_T^2 \rangle$. For the structure function alone it would be sufficient to take it as q^2 . Whereas k_{min}^2 follows trivially from zero angle gluon emission kinematics, k_{max}^2 is given by the requirement that the gluon can be recognized to form a jet with quark k . In other words, the apparent jet axis should be the direction of quark p . This is fulfilled if we demand $(1 = \text{gluon momentum})$ in the CMS

$$\star(\vec{k}, \vec{\ell}) \leq \star(\vec{p}, \vec{\ell}) \quad (2.10)$$

and

$$\star(\vec{k}, \vec{\ell}) \leq \star(\vec{k}, \vec{p})$$

We shall not write down the formula for k_{max}^2 , but note that $k_{max}^2 \rightarrow k_{min}^2$ for $x \rightarrow 1$ in contrast to full phase space.

For the running coupling constant $\alpha_s(k^2)$ we assume four active flavours such that at large k^2

$$\alpha_s(k^2) = \frac{4\pi}{8.33 \ln k^2/\Lambda^2} \quad (2.11)$$

We set $\Lambda = 500$ MeV and, since we cannot tolerate singularities in the region of integration, have modified (2.11) in an uninteresting way for $k^2 \lesssim M_0^2$.

Now we have to specify the inhomogeneous function $W_0(x, k^2)$. It describes i) all gluon contributions, real and virtual, connected to quark p, ii) virtual corrections to the quark-photon vertex.

Since the latter, in axial gauge, do not depend on k^2 , we simply can set

$$W_0(x, k^2) = \rho(x) Z(q^2). \quad (2.12)$$

The function $\rho(x)$ is given by the mass spectrum of the p-jet, since, for $k^2 \ll q^2$,

$$p^2 = q^2(1-x). \quad (2.13)$$

We shall determine this mass spectrum from that of the k-jet (setting $\rho(x) = \delta(1-x)$ as a first approximation). The normalization factor $Z(q^2)$ can be fixed by the requirement that the total cross section

$$\sigma_{tot} = \int_0^1 dx W(x, \rho) \quad (2.14)$$

(which is true here as we neglect quark pair creation via gluons) equals the QCD-result (10). For inclusive distributions it is irrelevant.

The solution of (2.7) has to be renormalized by an "external" propagator $d(x, M_0^2, \epsilon)$, which differs from (2.5) because of our specific cut-off procedures in (2.7) and (2.8). This propagator can be derived in the

following way. The exponent in (2.5) is the dispersion integral over k'^2 of the gluon emission probability from a quark with virtuality k^2 . The special form of the argument of the logarithm in (2.5) is the consequence of the term $x'k'^2/xq^2$ in (2.9), which renders the x' -integration in (2.7) finite at $x' = 1$ even for $\epsilon = 0$ (taking $k^2 = 0$) (6). For finite ϵ this x' -cut-off is only active for $k'^2/xq^2 > \epsilon$. If we split the k'^2 -integral into a piece from M_0^2 to ϵxq^2 and another from there to q^2 , only the first one has a strong x -dependence, which leads to

$$d(x, M_0^2, \epsilon) = \text{const} \exp\left(-\frac{4}{3\pi} \alpha_s(\hat{k}^2) \ln \frac{1}{\epsilon} \ln x\right) \quad (2.15)$$

where $M_0^2 < \hat{k}^2 < \epsilon xq^2$.

With this function we have to multiply the solution of (2.7), which leads to an enhancement for small x . Since the above considerations are admittedly qualitative, we shall discuss the effect of (2.15) separately in the results.

The BSE (2.7) can be solved by iteration, since because of $k_{\min}^2 \sim k^2$ the convergence is exponential. We see, however, that its first iteration does not agree very well with the exact first order expression (11)

$$\frac{1}{\sigma_0} \frac{d\sigma_1}{dx dx'} = \frac{2 \alpha_s(\hat{k}^2)}{3\pi} \frac{x^2 + x'^2}{(1-x)(1-x')} \quad (2.16)$$

where $k^2 = q^2(1-x')$. Especially for $x \approx x'$ the first iteration of (2.7) gives cross sections which are substantially smaller than (2.16). We therefore replaced the kernel in (2.7) by the r.h.s. of (2.16) for the first iteration.

3. Numerical results

In order to perform the higher dimensional integrals encountered in solving (2.7), we expanded $W(x, k^2)$ into a set of orthogonal polynomials. The actual variables differed from k^2 and x^1 by logarithmic mappings to deal with the almost singular behaviour at the limits $k^2 \rightarrow 0$ and $x^1 \rightarrow 1$. The iteration of (2.7) then reduces to matrix multiplication, and a 7×7 dimensional basis was found to give sufficient ($\sim 5\%$) accuracy.

The average k_T^2 of quark k with respect to the jet axis (as given by quark p) can be found only approximately in higher orders. For the first iteration we can weight the integration in (2.7) by $\sin^2 \vartheta_1$ with $\vartheta_1 = \vartheta(\vec{k}, \vec{p})$. After the first iteration, however, the information about the direction of \vec{p} is lost. We therefore can only calculate, for the n -th gluon emission, the average $\langle \sin^2 \vartheta_n \rangle$ with $\vartheta_n = \vartheta(\vec{k}, \vec{k}')$. Then at large x , where the quark deflection angles are small, the approximation

$$\langle k_T^2 \rangle \approx X^2 \frac{q^2}{4} \sum_{n=1}^{\infty} \langle \sin^2 \vartheta_n \rangle \quad (3.1)$$

for the average quark k_T^2 is quite good.

We first describe the results for the quark inclusive spectra and $\langle k_T^2 \rangle$, which both are cut-off dependent. We concentrate on two values of $\sqrt{q^2} = 12$ GeV and 30 GeV. For the cut-off mass M_0^2 in (2.7) we choose either $M_0^2 = 1$ GeV² or 2 GeV², and ϵ in (2.8) was fixed as $\epsilon = 0.01$. For a large part of our calculations we have omitted the external propagator renormalization (2.15), as we regard its detailed form somewhat speculative. Its effect shows up in the quark inclusive spectra and in the hadronic $\langle p_T^2 \rangle$.

First of all the mass spectrum of the k -jet, which determines the "Born term" (2.12), is found to be well described by

$$\begin{aligned} \rho_k(k^2) &\approx 1/(\delta + k^2/q^2)^2 \\ \text{or} \\ \rho(x) &\approx 1/(1 + \delta - x)^2 \end{aligned} \quad (3.2)$$

with $\delta \approx 0.016$. This corresponds, at $\sqrt{q^2} = 30$ GeV, to a mean squared jet mass $\langle k^2 \rangle = 42$ GeV². The deviation of $\rho(x)$ from a δ -function is almost irrelevant.

In fig. 2a we show inclusive quark spectra normalized to the same area as a function of x for the two values of q^2 and M_0^2 . It is evident that gluon radiation does not decelerate the leading quark severely. Even for $M_0^2 = 1$ GeV² it loses in the average only 1/3 of its energy. The dotted curve in fig. 2a gives $W(x, 0)$ for $M_0^2 = 1$ GeV², $\sqrt{q^2} = 30$ GeV after inclusion of $d(x, M_0, \epsilon)$ of (2.15) with $\tilde{k}^2 = 0.6\epsilon q^2$. One obtains a rather flat spectrum which means that $\langle x \rangle \approx 0.5$. Since this is still a moderate energy loss, the naive quark parton picture is not strongly modified in higher orders. Clearly the quark spectrum becomes softer if we raise q^2 or lower M_0^2 . Whereas the former phenomenon is the standard scaling violation, the second one is harmless as it can be absorbed into the unknown fragmentation function of quarks into hadrons (12).

Likewise the dependence of $\langle k_T^2 \rangle$ on M_0^2 as plotted in fig. 2b is mainly a consequence of the change in the quark energy spectrum due to collinear gluon emission. It produces no significant change in hadronic $\langle p_T^2 \rangle$, if the quark fragmentation is changed such that the hadronic spectrum remains invariant.

Let us turn to the results for hadronic $\langle p_T^2 \rangle$. Of course these depend on how the quarks fragment into pions (we disregard all complications due to different flavours and hadron species). In principle we can, for a given M_0^2 , fit the fragmentation function $D(z)$ to the inclusive hadronic spectra $d\sigma_x/dx$ at

high q^2 by setting

$$\frac{d\sigma_k}{dx} = \int_x^1 \frac{dz}{z} D(z) W\left(\frac{x}{z}, 0\right) \quad (3.3)$$

Unfortunately the available data are not precise enough, especially for $x > 0.6$, to allow a good determination of $D(z)$. Our speculative ansatz will therefore be revised, when better spectra are available. We choose, for $M_0^2 = 1 \text{ GeV}^2$,

$$D(z) = \text{const} \frac{1-z}{z} (1 - 1.3(z - z^3)) \quad (3.4)$$

in order to get approximately an exponential spectrum with a spike at small x . In fig. 3 we compare $d\sigma_k/dx$ from (3.3) for $\sqrt{q^2} = 30 \text{ GeV}$ with a recent calculation (13), where we have included the gluonic contribution calculated in a Monte Carlo iteration of (2.7). Since $W(x,0)$ still has a peak at $x \rightarrow 1$, the behaviour of $d\sigma_k/dx$ for $x \rightarrow 1$ is complicated and lies between const $(1-x)^2$ and const $(1-x)$. The propagator (2.15) has not been included in fig. 3.

If $W_1(x,0)$ is the function obtained from (2.7) by weighting with k_T^2 under the integral ($W_0(x,0)$ has $\langle k_T^2 \rangle = 0$), we obtain for the hadronic transverse momenta

$$\langle P_T^2(x) \rangle = \int_x^1 z dz D(z) W_T\left(\frac{x}{z}, 0\right) / \frac{d\sigma_k}{dx} \quad (3.5)$$

This function is shown in fig. 4a for the two values of q^2 . For $\sqrt{q^2} = 30 \text{ GeV}$ we compare it to the $O(\alpha_s)$ result (5), calculated with a sharp cut-off in k_T^2

at $M_0^2 = 45 \text{ GeV}^2$ and with the argument of α_s taken as q^2 . Of course $D(z)$ has to be readjusted to give the same $d\sigma_k/dx$. We see that for $x > 0.5$, where our approximations are reliable, higher order gluon emission increases $\langle P_T^2(x) \rangle$ by more than 30 %, if we neglect $d(x, M_0^2, \epsilon)$. When this propagator renormalization is included, the predictions for $\langle P_T^2(x) \rangle$ are almost a factor of 2 above the $O(\alpha_s)$ calculation. The origin of this effect is the suppression of the large x part of $W(x,0)$, where $\langle k_T^2 \rangle$ is small. Our curves do not contain any nonperturbative contribution to $\langle P_T^2 \rangle$, about the x -dependence of which nothing is known.

The last point deals with the separation of the two jets of each annihilation event according to which has the bigger $\langle P_T^2 \rangle$. Such a separation has been performed in the experimental analysis (1,2), and it drastically enhances the bremsstrahlungs effects due to the large fluctuations in $\langle P_T^2 \rangle$. We shall perform a similar analysis by taking the jet masses p^2 and k_1^2 as a measure for the "width" of a jet, where k_1 is indicated in fig. 1a. Would we ignore mass generation by fragmentation completely, the inhomogeneous term $W_0(x, k^2)$ in (2.7) would never contribute to the wide jet, which would overestimate $\langle P_T^2 \rangle$ for the wide jet. A more realistic separation of $W_0(x, k^2)$ will be attempted as follows. Based on hadronic multiplicity and transverse momenta we assume a nonperturbative mass distribution for $W_0(x, k^2)$

$$\rho_{m.p.}(k^2) = k^2 e^{-k^2/20 \text{ GeV}^2} \quad (3.6)$$

at $\sqrt{q^2} = 30 \text{ GeV}$. This and the mass distribution (3.2) let about 25 % of $W_0(x, k^2)$ contribute to the wide jet. We have checked that our selection of the wide jet gives exactly one half of the integrated inclusive cross section.

In fig. 4b we show, for $\sqrt{q^2} = 12$ and 30 GeV, the results for $\langle p_T^2(x) \rangle$ of the wide jet both for the full solution and for the $O(\alpha_s)$ calculation. For $\sqrt{q^2} = 30$ GeV we also include the propagator renormalized curve. Some large x experimental points from PETRA (ref. (1)) around $\sqrt{q^2} = 30$ GeV are indicated. These should not be compared directly to the theoretical curves, as they are not corrected for radiative and other effects, whereas the latter do not contain the nonperturbative effects. The spread between the theoretical predictions is, as for the overall $\langle p_T^2 \rangle$, almost a factor 2 around $x = 0.6$. Whether in this region the version with propagator renormalization is still compatible with experiment cannot be answered with the present statistical errors. The narrow jet also receives a contribution to $\langle p_T^2 \rangle$ which, however, is very sensitive to how we split the inhomogeneous part $W_0(x,0)$ according to (3.6). At $\sqrt{q^2} = 30$ GeV the maximal contribution is about $0.2 \text{ GeV}^2/c^2$ at $x = 0.5$.

4. Conclusions

We have solved the Bethe-Salpeter equation for multigluon emission in the ladder approximation numerically. A low value for the cut-off $M_0^2 = 1 \text{ GeV}^2$ has been used. This makes gluon emission a likely process in the sense that the quark loses in the average 1/3 to 1/2 of its energy to gluons. When a phenomenological quark fragmentation function is adjusted to yield a reasonable hadronic inclusive spectrum, the full solution gives values for squared hadronic transverse momenta which are almost a factor 2 higher than the $O(\alpha_s)$ calculation. Besides the obvious ambiguity due to the choice of the fragmentation function it should be clear that our basic equation (2.7) is a very approximate one.

Terms of the order k^2/q^2 have been neglected almost everywhere, and this ratio is not very small especially for the high k_T gluon emission events. The selection of ladder type Feynman diagrams is also questionable on this level of accuracy. Thus it may be that the differences between a more complete higher order calculation and the $O(\alpha_s)$ result are not as large as we have found.

Although our method of solution of the Bethe-Salpeter equation is quite efficient for determining $W(x,k^2)$, it is not easily applicable to calculate average quantities which do not simply add in each order, e.g. other moments of p_T . This will be improved in future work by introducing more integration variables.

Acknowledgement

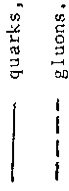
Numerous discussions with Dr. E. Pietarinen and Prof. S. Pokorski have been extremely helpful.

References

- 1) TASSO-Collaboration, R. Brandelik et al., Phys. Lett. 86B (1979) 243
- 2) PLUTO-Collaboration, Ch. Berger et al., Phys. Lett. 86B (1979) 418
- 3) MARK J-Collaboration, D.P. Barber et al., Phys. Rev. Lett. 43 (1979) 418
- 4) JADE-Collaboration, W. Bartel et al., DESY 79/77 (November 1979)
- 5) P. Hoyer, P. Osland, H.G. Sander, T.F. Walsh and P.M. Zerwas, Nucl. Phys. B161 (1979) 349
- 6) Y.I. Dokshitser, D.I. Dyakonov and S. Troyan, Proceedings of 13th Winter-school, Leningrad 1978 (SLAC-TRANS-183), to appear in Physics Reports. L.N. Lipatov, Yad.fiz. 20 (1974) 181. V.N. Gribov and L.N. Lipatov, Yad.fiz. 15 (1972) 781, 1218.
- 7) W.R. Frazer and J.F. Gunion, Phys. Rev. D19 (1979) 2447
- 8) D. Amati, R. Petronzio and G. Veneziano, Nucl. Phys. B146 (1978) 29
- 9) G. Altarelli and G. Parisi, Nucl. Phys. B126 (1977) 298
- 10) T. Appelquist and H. Georgi, Phys. Rev. D8 (1973) 4000; A. Zee, Phys. Rev. D8 (1973) 4038
- 11) J. Ellis, M.K. Gaillard and G. Ross, Nucl. Phys. B111 (1976) 253; T. DeGrand, Y.J. Ng and S.-H. Tye, Phys. Rev. D16 (1977) 3251
- 12) R.K. Ellis, H. Georgi, M. Machacek, H.D. Politzer and G. Ross, Nucl. Phys. B152 (1979) 285
- 13) TASSO-Collaboration, R. Brandelik et al., DESY 79/73 (November 1979)

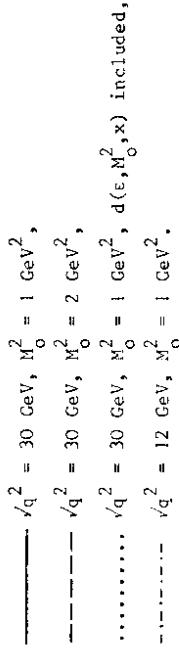
Figure Captions

Fig. 1 a) Tree diagrams for gluon emission,



b) Bethe-Salpeter equation for quark structure function, generating tree diagrams.

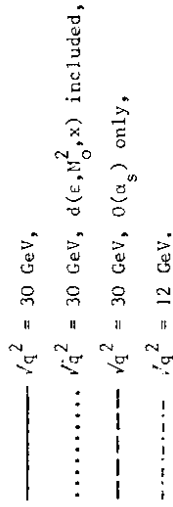
Fig. 2 a) Inclusive spectra for quarks (arbitrary normalization)



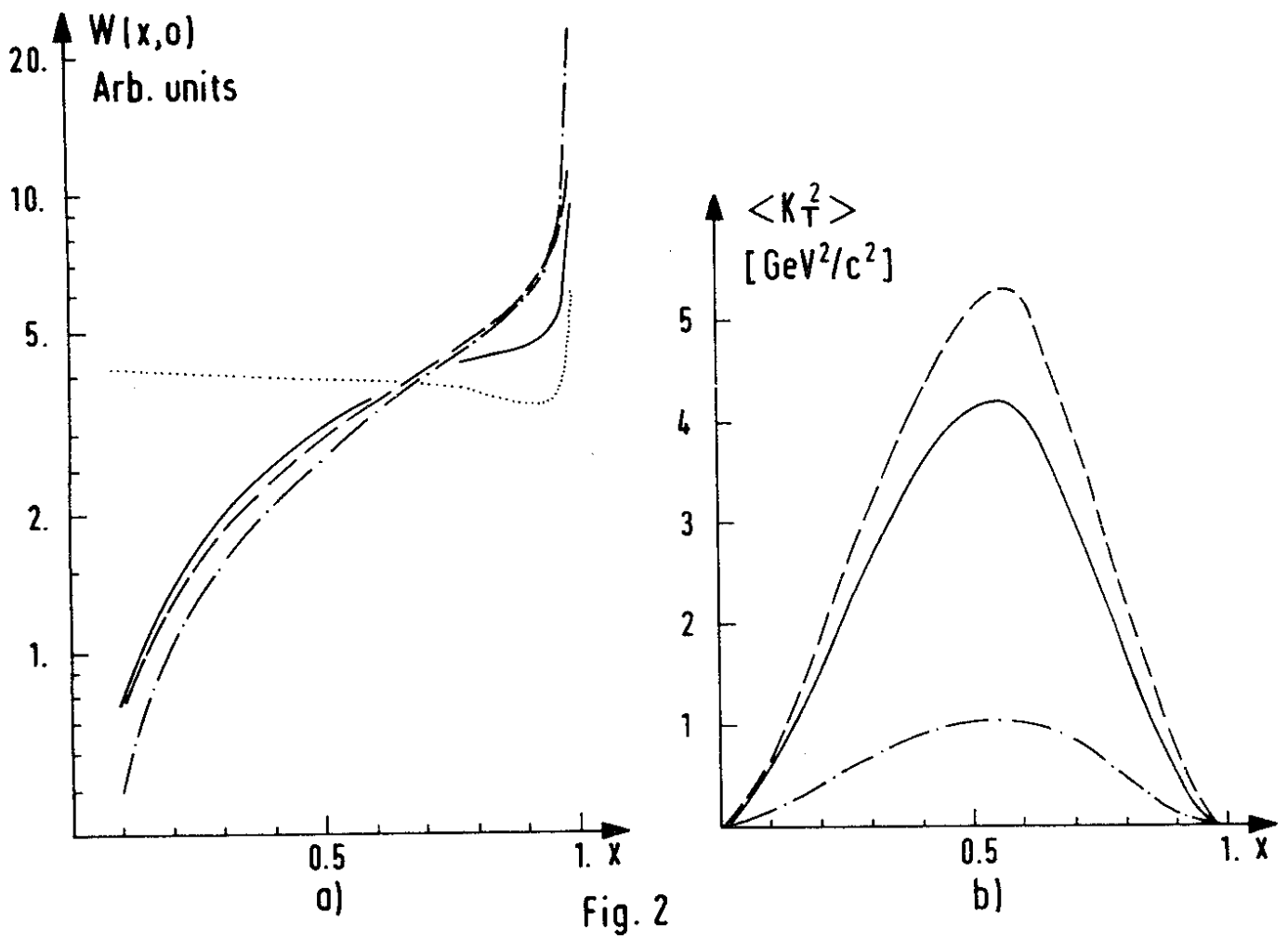
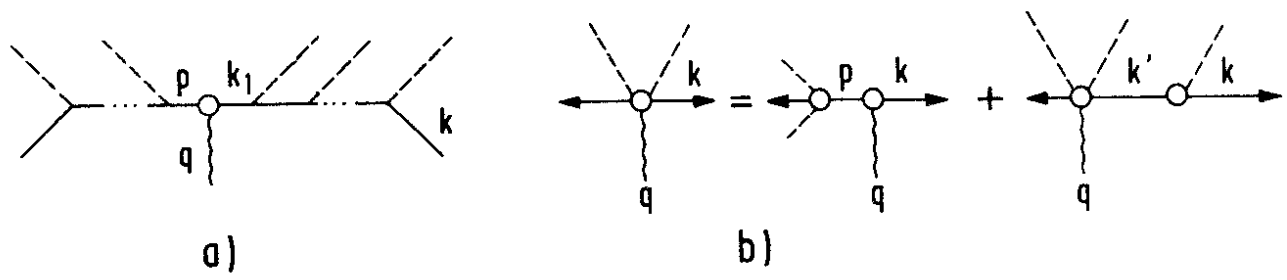
b) $\langle k_T^2 \rangle$ for quarks. Curves have the same meaning as before.

Fig. 3 Fit to hadronic inclusive spectra at $\sqrt{q^2} = 30 \text{ GeV}$. Data are from ref. (13).

Fig. 4 a) $\langle p_T^2 \rangle$ for hadrons, $M_0^2 = 1 \text{ GeV}^2.$



b) $\langle p_T^2 \rangle$ for hadrons, wide jet. Curves have the same meaning as before.



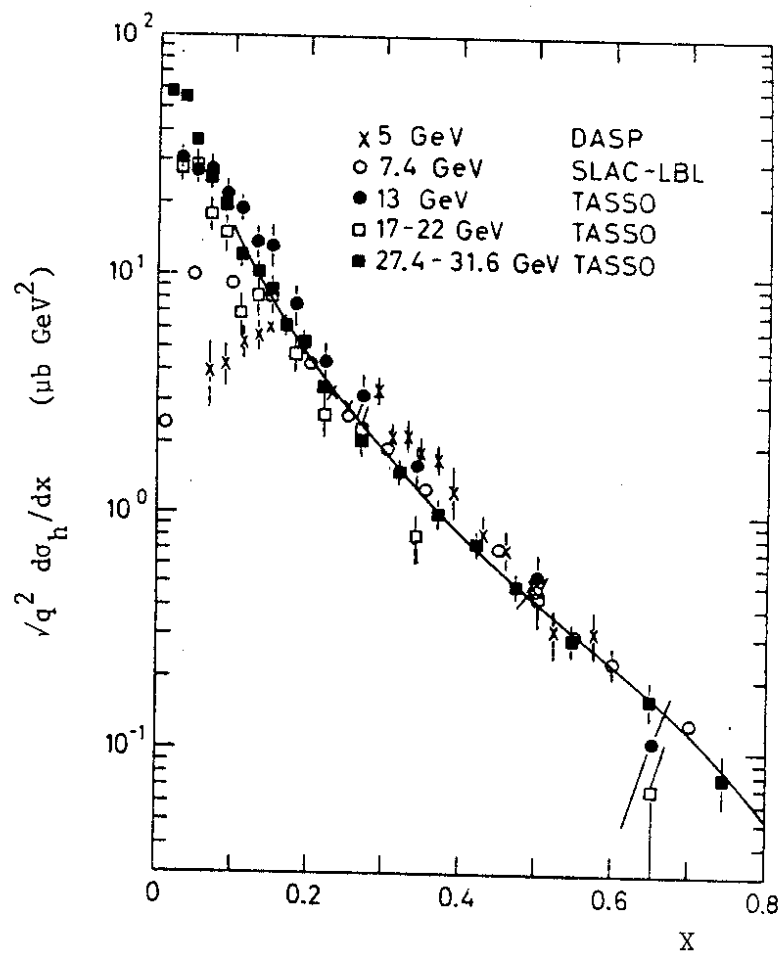


Fig. 3

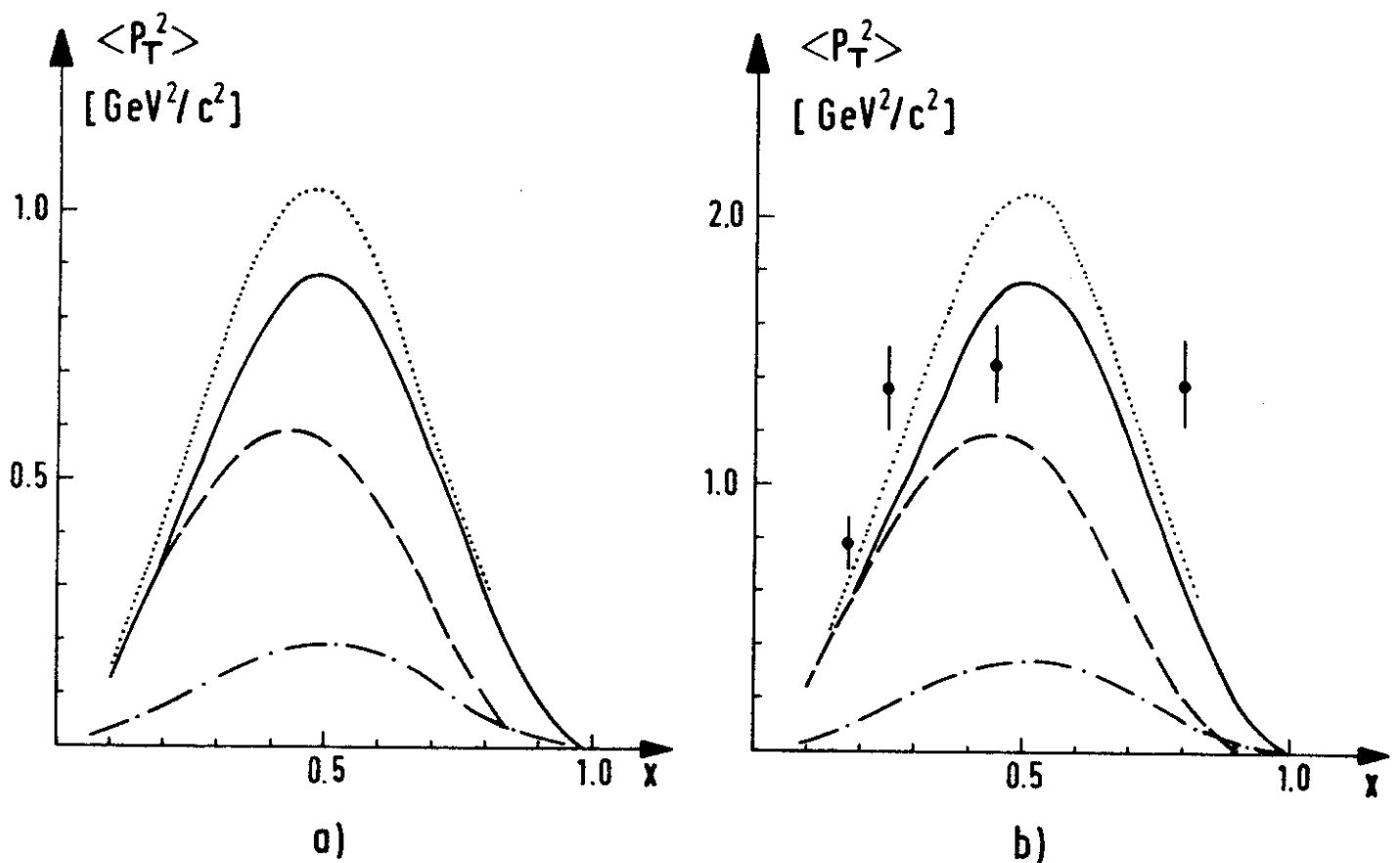


Fig. 4